

Full Length Research Paper

Synthesis of Cu-Ag core-shell particles: Study on cover silver homogeneity

Yu-hsien Peng^{1,2*} and Ching-Hwa Lee¹

¹Department of Environmental Engineering, Dayeh University, 168 University Rd., Dacun, Changhua, Taiwan 515 ROC.

²Department of Research and Development, Oriental Happy Enterprise Co., No.27, Xin'ai Rd., South Dist., Tainan, Taiwan 702 ROC.

Accepted 20 December, 2011

Cu-Ag particles with homogeneous cover-silver layer were synthesized by electroless plating of copper particles with silver sulfate using eco-friendly sodium citrate (SC) as reducing agent, dispersant and chelating agent in an aqueous system. The influences of sodium citrate/Cu and sodium citrate/Ag ratios on Ag coatings of Cu powders were investigated. Ag formed a dense coating on the surface of Cu powders at a molar ratio of SC/Cu=0.25/1 and SC /Ag=8/1. SEM (scanning electron microscopy) showed a uniformity of Ag coatings on Cu powders. SEM images and EDS (The energy dispersed spectrometry) analyses also revealed that Cu cores were covered by Ag shells on the whole. The measurement of oxidation resistance of Cu-Ag particles shows closer resistivity ($6.25 \times 10^{-4} \Omega \cdot \text{cm}$) than pure Ag ($9.25 \times 10^{-5} \Omega \cdot \text{cm}$) without CuO (-1 1 1) and Cu₂O (1 1 1) and peaks were detected after heat-treatment at 350°C for 4 h.

Key words: Cu-Ag particles, electroless plating, oxidation resistance.

INTRODUCTION

Silver and copper are widely used in many fields such as electronic industries (Lee et al., 2008; Park et al., 2007), sensors (Athanassiou et al., 2006), catalysis (Ranu et al., 2007), and optical or biological devices due to their high electrical conductivity. Because of the rare content of silver in the earth's crust and easy oxidization of copper, their applications is strongly limited. Thus, Cu-Ag core-shell (Cu-Ag) particles instead of single copper or silver particles is currently considered to be an advisable option in electronic industry in order to solve the above problems (Hai et al., 2006).

Generally speaking, particles with core-shell structure can be synthesized by vacuum process such as evaporation, sputtering (Wang et al., 1997), electroplating (Takeshima et al., 1990) and electroless plating (also called spontaneous displacement reaction) (Feldstein, 1981), etc. It is widely accepted that silver can be deposited

on many substrates by electroplating (Vaskelis et al., 1996). However, electroplating and vacuum processes are not feasible for commercial purposes depending on the efficiency of the particles which is extremely low. The spontaneous displacement reaction of silver coating that can be achieved on copper particle has a higher deposition rate than electroplating, although there are still difficulties in the reducing process steps which forms a well silver coating on the surface of copper particle. According to literature, the rate of replacement reaction is very important and it has great impact on the final product. Xu et al. (2003) reported a synthesis of silver coating on fine copper particle via Cu displacement with silver nitrate/ ammonium hydroxide solution. The quantity of ammonia controlled the rate of copper dissolution. Mancier et al. (2010) prepared the Cu-Ag core-shell nanoparticles by ultrasound-assisted electrochemistry followed by a displacement reaction. Ethylenediaminetetraacetic acid (EDTA) was used as the chelating agent to control the rate of Ag-Cu displacement.

In the aforementioned references, many of these synthetic methods are difficult for mass-production scale due to their low efficiency or the inadequacy of precious

*Corresponding author. E-mail: D9805003@mail.dyu.edu.tw, pengyuhsien@hotmail.com. Tel: 886-4-851-1338, 886-6-261-8328. Fax: 886-6-2616003.

equipment. Furthermore, in most of the processes, sodium borohydride (NaBH_4), hydrazine hydrate ($\text{N}_2\text{H}_4 \cdot \text{H}_2\text{O}$) were used as reducing agent, hexadecyltrimethyl ammonium bromide (CTAB), polyvinylpyrrolidone (PVP) and Ethylenediaminetetraacetic acid (EDTA), etc. were used as dispersant and chelating agent, respectively, which are poisonous or hard to be removed from the final products. Recently, sodium citrate ($\text{Na}_3\text{C}_6\text{H}_5\text{O}_7$) was found to be more widely used for replacing the above chemicals as multifunctional agent (Teramoto et al., 2000; Yang et al., 2010), such as a reducing, dispersant, chelating agent, etc., and it also suppresses the precipitation of copper hydroxides in Cu-Ag spontaneous displacement reaction (Boca et al., 2009; Gils et al., 2010; Kumar and Reddy, 2010; Xu et al., 2003; Yang et al., 2010).

In this paper, we reported a simple and novel method to synthesize Cu-Ag particles using silver sulphate, copper particles, SC (Sodium citrate) as starting materials at room temperature. As compared with the results reported previously, this method is a relatively green synthetic method because the starting materials come from SC which serve as a multifunctional agents such as reducing agent, dispersant and chelating agent, and are nontoxic and easily available. Furthermore, the Cu-Ag particles prepared by this method have greater potential for application in many fields.

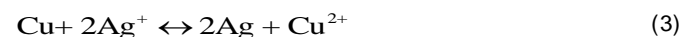
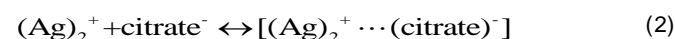
MATERIALS AND METHODS

Materials

Silver sulphate (Ag_2SO_4) was gotten from Solar Technology Inc., Taiwan, SC ($\text{Na}_3\text{C}_6\text{H}_5\text{O}_7$) was from Union Chemical Works Ltd., Taiwan, copper particles with median size $7.36 \mu\text{m}$ was supplied by Oriental Happy Enterprise Co., Ltd., Taiwan. All chemicals were used as received without further purification.

Preparation of Cu-Ag particles

The chemical reactions of copper particles, SC and Ag_2SO_4 systems occurs as shown in Equation (1) to (4) (Djokić, 2008; Vaskelis et al., 1996).



During the preparation of Cu-Ag particles, two solutions denoted as A and B were first prepared. For preparing solution A, 2.53 g Cu particles, 0.09 g SC and 100 ml of deionized water were mixed at room temperature by a magnetic stirrer; for preparing solution B, 1.17 g Ag_2SO_4 , various amounts of

SC and 250 ml of deionized water were mixed to form $[(\text{Ag})_2^+ \cdots (\text{citrate})^-]$. Detailed experimental design was shown in Table 1. First, solution B was quickly dropped into solution A with a magnetic stirrer at 1000 rpm. After the color of the reacting solution change from red to purple and then dark green, the reaction was ended by stopping the motion of the magnetic stirrer which was immediately followed by the filtration and cleaning process. The obtained composite particles after single step filtration were washed at least 3 times with deionized water, and then dried.

Preparation of metal paste

To ascertain the oxidation resistance of synthetic powder, the resistivity (ρ) of synthetic powders were investigated. The prepared particles were mixed with an appropriate amount of ethyl acetate-terpineol solution by a three-roll mill. The paste was grounded to the required consistency, and screened on the glass substrates for forming metal films, and then dried in various conditions at air ambient.

Characterization

The morphologies of the synthetic particles were observed by scanning electron microscopy (SEM) (SEM, JEOL JSM-7001F, Japan). The median size (D_{50}) of the particles was estimated with a laser particle-size analyzer (DLS, Beckman Coulter, Germany). The phase composition of the prepared particles was determined by X-ray diffraction (XRD, DX-2500, Mainland China) using $\text{CuK}\alpha$ radiation ($\lambda = 0.1542 \text{ nm}$). The energy dispersed spectrometry (EDS) of SEM (samples of $[\text{SC}]/[\text{Cu}] = 0.25$ and $[\text{SC}]/[\text{Ag}] = 8$) and inductively coupled plasma – optical emission spectrometer (ICP-OES) were also used for the element identification of the products. The oxidation resistance of synthetic particles was tested by measuring sheet resistance of metal films which changed with the various conditions of heating time and ambient temperature. The sheet resistances of metal films were measured with a programmable milli-ohm meter (ABM-3245) on samples which have $10 \times 10 \text{ mm}^2$ metal film patterns.

RESULTS AND DISCUSSION

Effects of $[\text{SC}]/[\text{Cu}]$ and $[\text{SC}]/[\text{Ag}]$ ratios on Cu-Ag particles synthesis

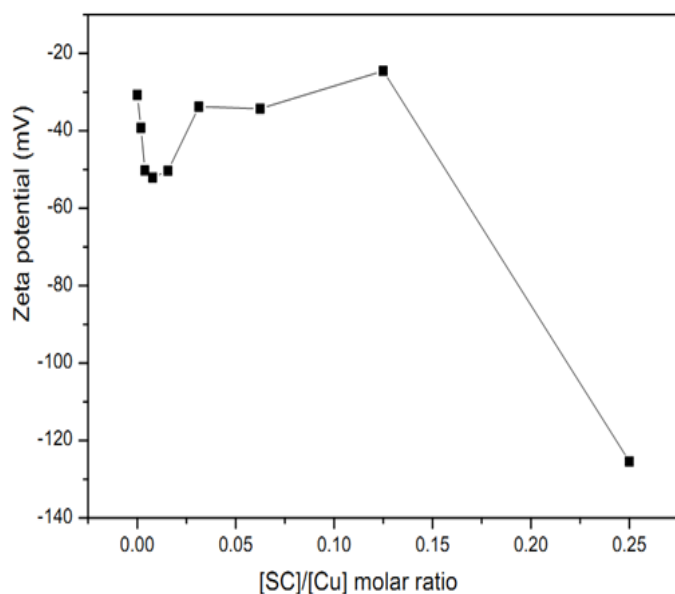
From the aforementioned functions of SC in this study, the major influences of SC concentration on the synthesis of Cu-Ag particles can be divided into two parts: (1) effects of SC concentration on the Cu particles dispersion and (2) effects of $[\text{SC}]/[\text{Ag}]$ ratio on Cu-Ag spontaneous displacement reaction.

In the cause of finding the effects of SC concentration on the Cu particles dispersion, copper particles, various amounts of SC and 100 ml of deionized water were mixed to dissolve at room temperature with a magnetic stirrer, and then the zeta potential of surface particles was measured by Zeta Potential Analyser (ZetaPlus 2002, Brookhaven, USA).

Generally, when the measuring modulus of zeta potential is above -25 mV that can provide enough

Table 1. Experimental conditions and characteristics of Cu@Ag particles.

Sample	[Cu]/[Ag ⁺] molar ratio	Solution A			Solution B		
		[SC]/[Cu] molar ratio	Cu particles(g)	SC for dispersant(g)	0.015M Ag ₂ SO ₄ (ml)	[SC]/[Ag ⁺] Molar ratio	SC for chelating(g)
1 SC	5.3	0.25	2.53	0.09	250	32	9.6
2 SC	5.3	0.25	2.53	0.09	250	16	4.8
3 SC	5.3	0.25	2.53	0.09	250	8	2.4
4 SC	5.3	0.25	2.53	0.09	250	4	1.2
5 SC	5.3	0.25	2.53	0.09	250	2	0.6
6 SC	5.3	0.25	2.53	0.09	250	1	0.3
7 SC	5.3	0.25	2.53	0.09	250	0.5	0.15
8 SC	5.3	0.25	2.53	0.09	250	0	0
9 SC	5.3	0	2.53	0	250	0	0

**Figure 1.** Zeta potential of Cu particles surface at the different [SC]/[Cu] molar ratios.

electrostatic force to disperse particles (Hiemenz, 1986). As shown in Figure 1, the zeta potential increased when the [SC]/[Cu] molar ratio falls between 0 and 0.0078, and then decreased between 0.0078 and 0.125 but when the [SC]/[Cu] molar ratio was increased to 0.25, the highest modulus of zeta potential was measured (-125 mV). This phenomenon may be caused by the effect of electrolyte concentration. When the SC concentration increased, the electrical double layer will be compressed and then recharged. The addition of SC leads to an obvious increase of negative charge on Cu surface particles, indicating the chemical adsorption type it has. The measured results shows that the molar ratio of [SC]/[Cu]=0.25 can provide the highest electrostatic force for particles dispersion.

Figure 2 shows the relationship between the average particle size (D_{50}) of synthetic particles and different synthetic parameter of [SC]/[Ag] molar ratios that showed a straight line ($Y=6.923+0.06214X$, $R^2=0.9359$). This result strongly suggest that the D_{50} of synthetic particles was directly proportional to the [SC]/[Ag] molar ratio. It can be seen that the D_{50} of particles increases when the molar ratio of [SC]/[Ag] increased. This is probably due to the excess SC, which is adsorbed on the Cu-Ag surface and inversely cause the agglomeration of particles. This result is similar to the findings of Hackley's research (1997). The evidence will be determined later.

Figure 3 shows the relationship between the reaction time of spontaneous displacement of Cu by Ag and different synthetic parameter of [SC]/[Ag] molar ratios that showed a straight line ($Y=9.1659+4.07359X$, $R^2=0.9794$). This result indicate that the reaction time was directly proportional to the [SC]/[Ag] molar ratio. It has been shown that the required reaction time increased when [SC]/[Ag] ratio increased from 0.5 to 32. This result indicated that when SC is overdosed, the rate of Cu-by-Ag replacement reaction will reduce, and then bigger Cu@Ag will be formed by reducing the nucleation rate of silver.

Figure 4 shows the SEM images of Cu-Ag composite particles with different [SC]/[Cu] and [SC]/[Ag] molar ratio. In Figure 4a, smaller Ag particles with dendritic morphology were already separated from Cu particles if SC was not present. It can be clearly seen in Figure 4b that the Ag coating was insufficient on Cu surface with a molar ratio of [SC]/[Cu]=0.25 and [SC]/[Ag]=0. Figure 4c shows that more complete coated particles can be produced within the molar ratio of [SC]/[Cu]=0.25 and [SC]/[Ag]=8. Figure 4d shows that the size of Ag particles on Cu surface were between 50~150 nm. The results indicated that when SC was added, it may provide nucleation sites for Ag⁺ on the Cu surface, otherwise Ag particles will randomly be precipitated from the solution. Figure 4e shows the cross sectional

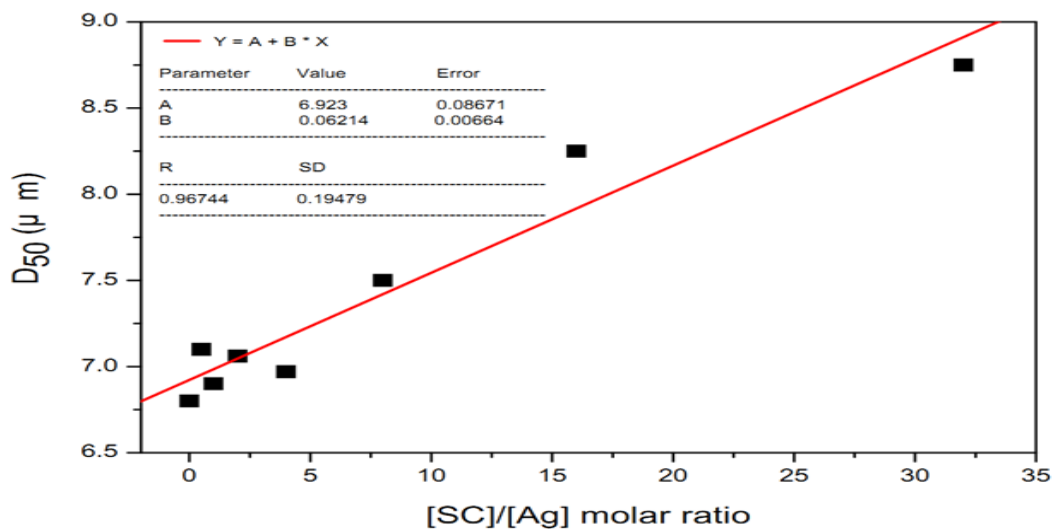


Figure 2. Tendency of Cu-Ag D_{50} with different [SC]/[Ag] molar ratios.

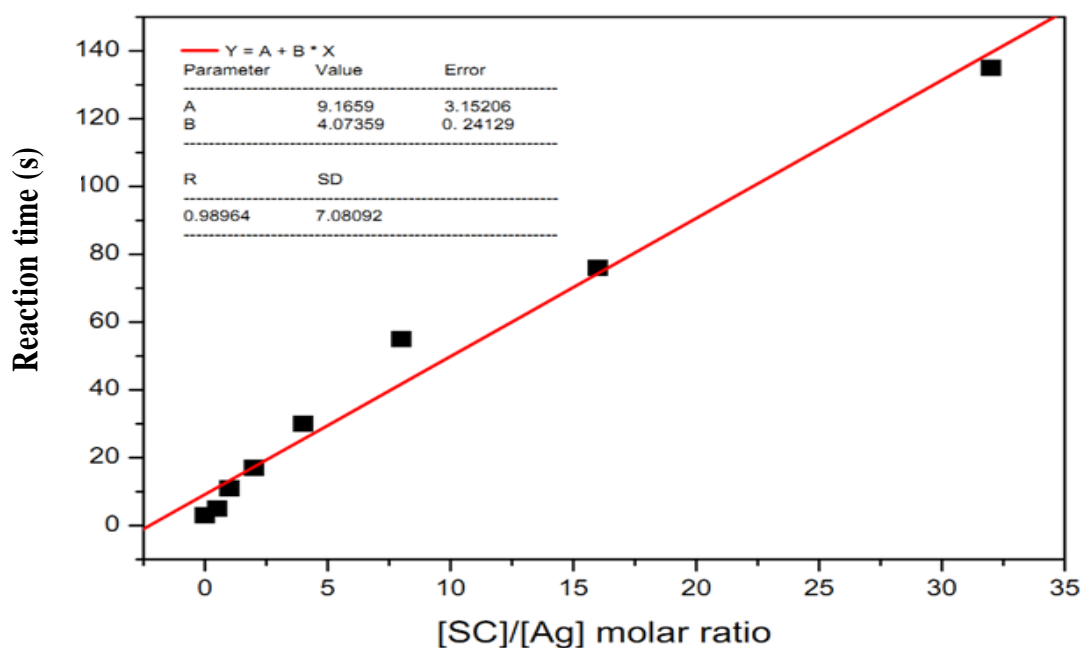


Figure 3. Tendency of the reaction time with different [SC]/[Ag] molar ratios.

image of synthetic particles. It can be clearly seen that each particles have a white shell of Ag and a dark core of Cu and the thickness of Ag layers were between 0.2~1.3 μm .

Table 2 summarizes the elemental analysis of silver and copper weight% of the synthetic particles by ICP-OES. As the results shown, the Cu-Ag particles contains 64.14~65.51 weight% of Cu, 34.49~35.86 weight% of Ag. It can be clearly seen, that the concentration of SC did not significantly affect the final reduction rate of silver and the loss rate of copper. The result

indicated that in the synthetic process, the SC only function as the dispersant and chelating agent, but not reducing agent. Further SEM-EDS analysis of Cu-Ag particles were also presented in Figure 5. Figure 5 shows the SEM-EDS analysis of the synthetic particles with molar ratio of [SC]/[Cu]=0.25 and [SC]/[Ag]=8 and contain small amount of oxygen and carbon, which were possibly introduced from three sources: (1) the adsorption of $\text{C}_6\text{H}_5\text{O}_7^-$ on synthetic powders surface, (2) oxidation of synthetic powders, or (3) background value from carbon conductive tape.

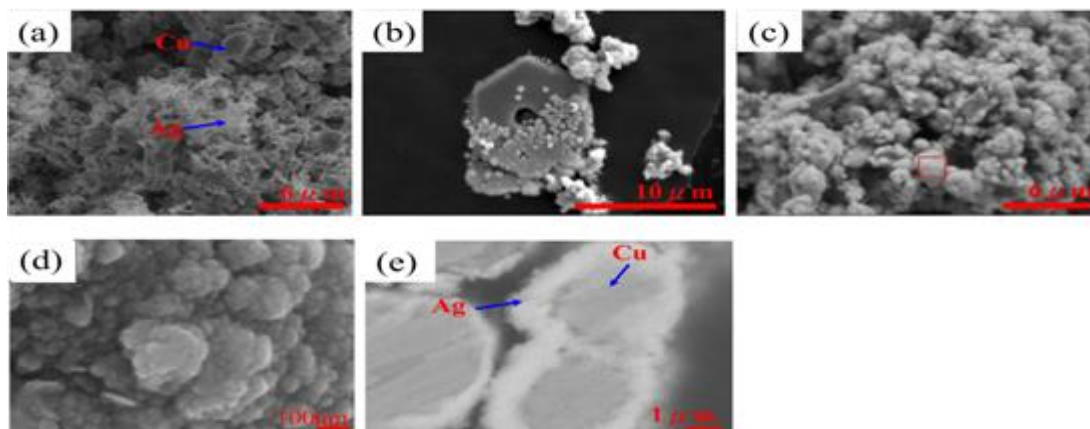


Figure 4. SEM images of Cu@Ag particles with (a) $[SC]/[Cu]=0$ and $[SC]/[Ag]=0$, (b) $[SC]/[Cu]=0.25$ and $[SC]/[Ag]=0$ (c) $[SC]/[Cu]=0.25$ and $[SC]/[Ag]=8$; (d) enlarged synthetic particles in selected area of (c), (e) cross section image of synthetic particles with $[SC]/[Cu]=0.25$ and $[SC]/[Ag]=8$.

Table 2. Elemental analysis of silver and copper wt% in Cu@Ag particles.

Sample	Cu (%)	Ag (%)
1 SC	65.41	34.59
2 SC	65.51	34.49
3 SC	65.39	34.61
4 SC	65.41	34.59
5 SC	65.46	34.54
6 SC	65.30	34.70
7 SC	65.14	34.86
8 SC	64.16	35.84
9 SC	64.18	35.82

To ascertain the surface adsorption of SC, the fourier transform infrared (FTIR) spectra were recorded on Cu-Ag particles as depicted in Figure 6. For comparison, the spectrum recorded for neat SC is also superimposed in the same figure. In Figure 6a, symmetric (ν_s) and asymmetric (ν_{as}) vibrations respectively emerged at the ranges of 1440-1350 and 1650-1550 cm^{-1} which correspond to a characteristic stretching vibration of COO^- groups. The bands between 2400-2375 and 3550-3300 cm^{-1} respectively correspond to a characteristic stretching vibration of C-O groups (from ambient air) and OH^- groups (H_2O). Figure 6b shows the presence of bands at 1410 and 1575 cm^{-1} which indicated that $\text{C}_6\text{H}_5\text{O}_7^-$ have existed on the particles surface.

The SEM cross-sectional image and EDS line-scan analysis were presented in Figure 7 for further analysis of synthetic powders. It can be clearly seen that in Figure 7b, the intensities of carbon and oxygen also detected an internal area of Cu-Ag powders and it can be determined as the background value in EDS analysis.

Oxidation resistance of Cu-Ag particles

A series of performance tests were carried out at 350°C for 4 h in ambient air on Cu-Ag particles. The x-ray diffraction (XRD) pattern of Cu-Ag particles have been recorded after different molar ratios of $[SC]/[Cu]$ and $[SC]/[Ag]$. Figure 8c to j shows the XRD pattern of Cu-Ag particles before heat treatment and only copper and silver were detected: Cu (1 1 1) orientation at 43.316°; Cu (2 0 0) at 50.448°, Cu (2 2 0) at 74.124° and Ag (1 1 1) orientation at 38.114°; Ag (2 2 0) at 64.441°, Ag (3 1 1) at 77.395° (Cu: JCPDS 04-0836, Ag: JCPDS 65-2871). Furthermore, It can be seen in Figure 8j that strong Ag (1 1 1) and Cu (1 1 1) peaks were identified with $[SC]/[Ag]=0$. The result is same as the SEM finding. When SC was not present, Ag and Cu particles both have strong peaks depending on complete structure. In Figure 4c-i, the peaks of Ag (1 1 1) were decreased when SC was added, and Cu (1 1 1) decreased with increasing $[SC]/[Ag]$ ratio, then increased when the molar ratio of $[SC]/[Ag]=16$ and 32. This phenomenon can be explained by adding SC which helps to form a silver coating on the copper powdered surface. Thus, when the Ag coating is dense and sufficient, the intensity of Cu (1 1 1) peaks decreased. Consequently, the Ag coating can be completely formed on Cu powders with $[SC]/[Ag]=8/1$.

Figure 9 shows the XRD pattern of Cu-Ag particles after heat treatment. Figure 9b, c, e, f, g, h and i shows the presence of the Cu_2O and CuO phase which was observed in the XRD pattern, indicating that Cu was partially oxidized at the molar ratios of $[SC]/[Ag]=32/1, 16/1, 4/1, 2/1, 1/1, 0.5/1$ and $0/1$. In Figure 9a, pure Cu particles were also tested and it presented stronger Cu_2O and CuO peaks than synthetic Cu-Ag particles. Table 3 summarizes the changes in intensity of CuO (-1 1 1) and Cu_2O (1 1 1)

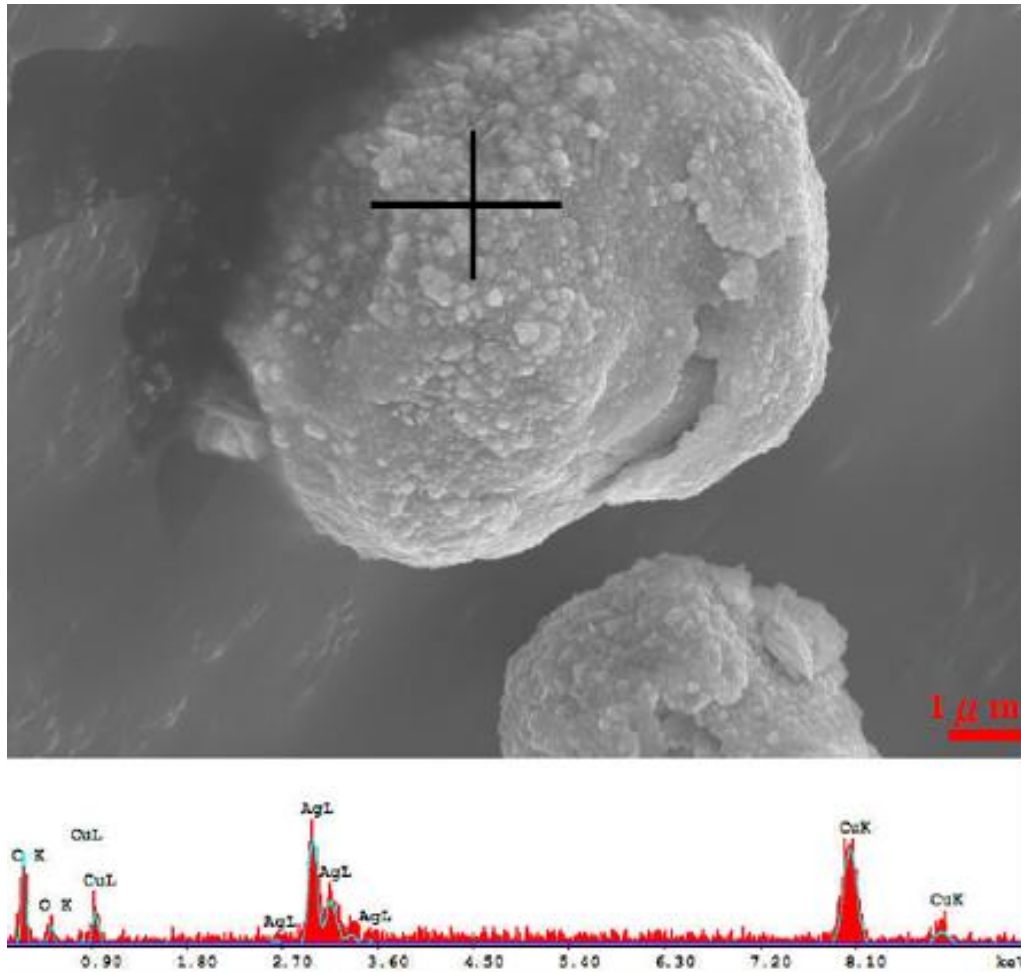


Figure 5. SEM micrograph of EDS analysis of Cu-Ag particles with $[SC]/[Cu]=0.25$ and $[SC]/[Ag]=8$.

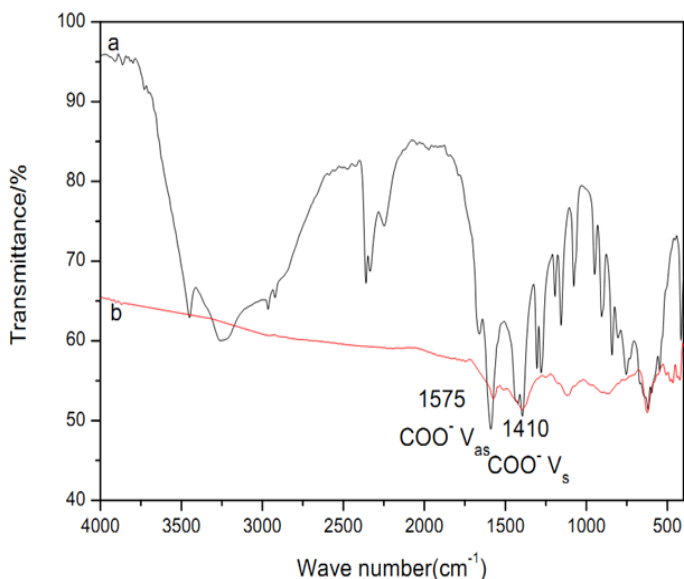


Figure 6. FT-IR spectra of (a) pure SC and (b) Cu-Ag particles.

peaks in Cu-Ag particles after heat treatment. The results show that when Cu-Ag particles were synthesized with the molar ratio of $[SC]/[Cu]=0.25$ and $[SC]/[Ag]=8$, no CuO (-1 1 1) and Cu_2O (1 1 1) peaks were detected. If the molar ratio of $[SC]/[Ag]$ was decreased to 4, then Cu_2O (1 1 1) peak with 129 intensity will be detected. Otherwise, when the molar ratio of $[SC]/[Ag]$ was increased to 16 or 32, CuO (-1 1 1) and Cu_2O (1 1 1) peaks will be performed together and the intensities will keep getting higher. This results indicate that when the molar ratio of $[SC]/[Ag]=4, 2, 1, 0.5$ and 1, the rate of Cu-by-Ag replacement reaction become too fast that Ag could not form a dense coating on the Cu surface. Furthermore, when the molar ratio of $[SC]/[Ag]=32$ or 16, then the rate of Cu-by-Ag replacement reaction can become slow, but too much adsorption of SC will cause a rare Ag coating.

A series of electrical performance tests were carried out on Cu-Ag powders with different $[SC]/[Ag]$ ratios. Heat-treatment in ambient air of printed patterns are necessary because it will remove the solvent that cause

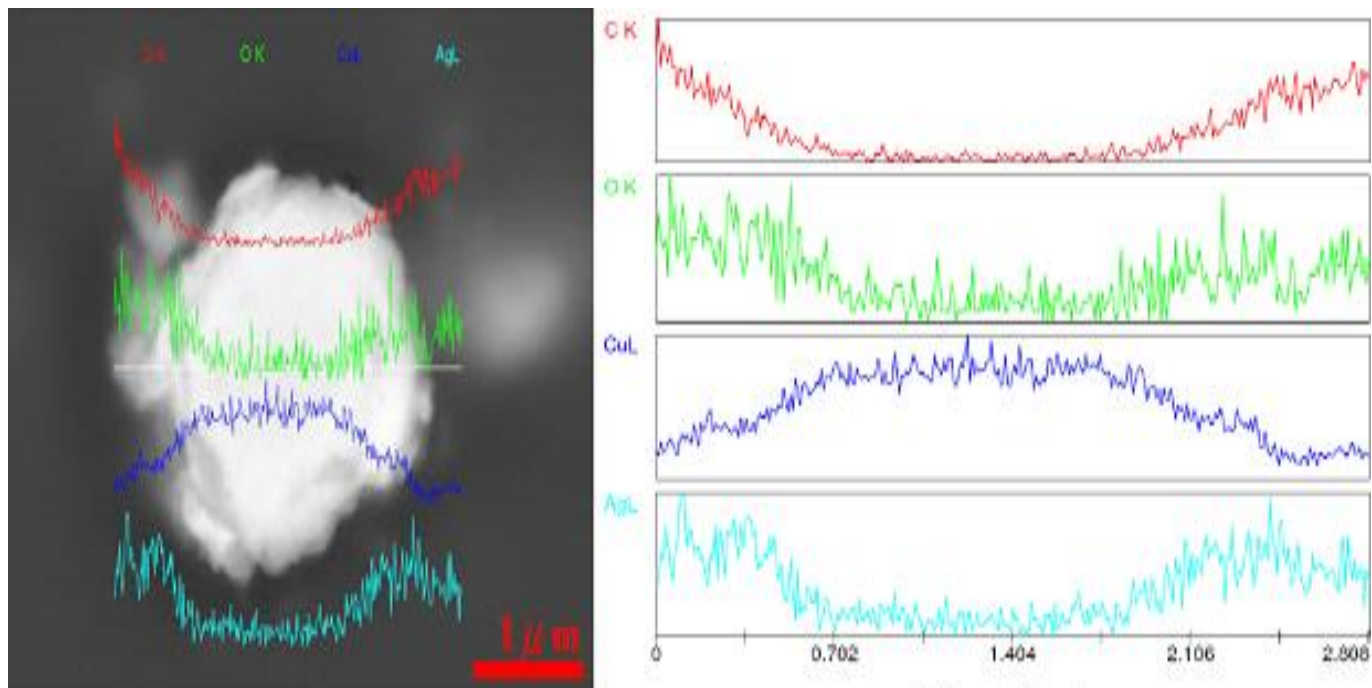


Figure 7(a). SEM cross-section image of Cu-Ag particles with $[SC]/[Cu]=0.25$ and $[SC]/[Ag]=8$, (b)EDS line-scan analysis of Cu-Ag particles with $[SC]/[Cu]=0.25$ and $[SC]/[Ag]=8$.

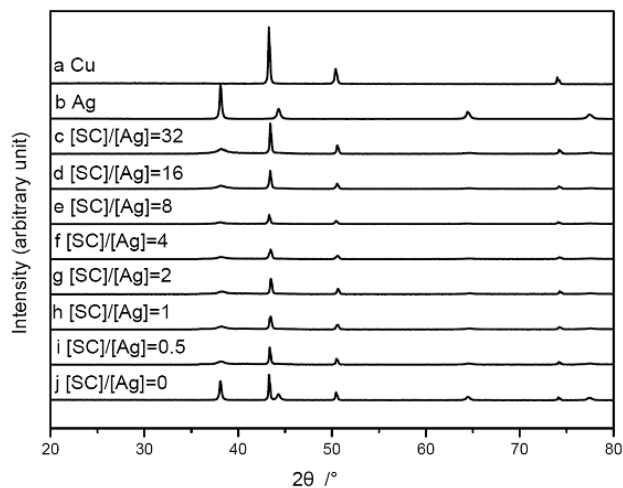


Figure 8. XRD patterns of Cu-Ag particles before heat treatment.

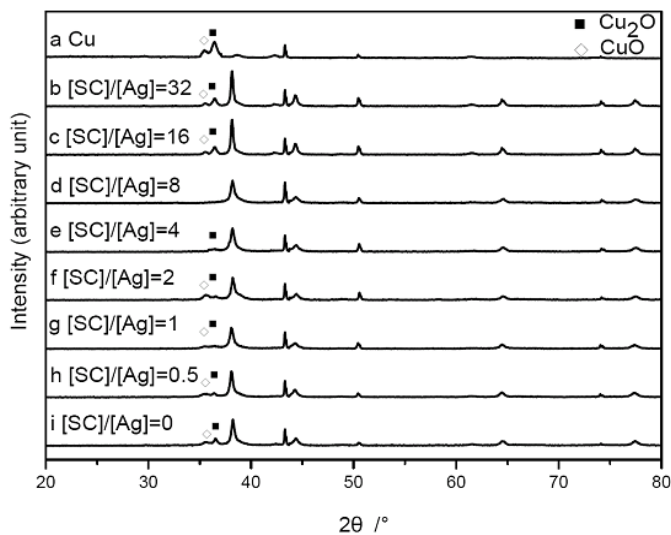


Figure 9. XRD patterns of Cu-Ag particle after 350°C 4 h heat treatment.

sintering between particles. Adjustment of the heat-treatment temperature of the printed patterns were exhibited in Figure 10. The resistivity of pure copper particles was too high ($15 \Omega \cdot \text{cm}$) as presented in Figure 10. After 50°C for 4 hrs heat treatment, the pure silver has the lowest resistivity which is $5.75 \times 10^{-4} \Omega \cdot \text{cm}$ and the resistivity of 1 SC to 8 SC are almost the same as $2 \times 10^{-3} \Omega$. The differences

between 1 SC to 8 SC cannot clearly be seen at 50°C for 4 h heat treatment except 9 SC. When the molar ratio of $[SC]/[Cu]=0$ and $[SC]/[Ag]=0$, then the resistivity of 9 SC is higher than others ($3.6 \times 10^{-1} \Omega$). This may be caused by separated particles of silver and copper, and the Cu will let the film resistivity to increase. Furthermore, the resistivity of 3 SC to 7 SC

Table 3. Effect of the thermal treatment of Cu@Ag particles.

Sample	Peak intensity			
	Before thermal treatment		After thermal treatment (350°C, 4 h in ambient air)	
	CuO (-1 1 1)	Cu ₂ O (1 1 1)	CuO (-1 1 1)	Cu ₂ O (1 1 1)
1 SC	0	0	104	408
2 SC	0	0	153	537
3 SC	0	0	0	0
4 SC	0	0	0	129
5 SC	0	0	240	113
6 SC	0	0	74	86
7 SC	0	0	132	159
8 SC	0	0	121	386
9 SC	0	0	530	982

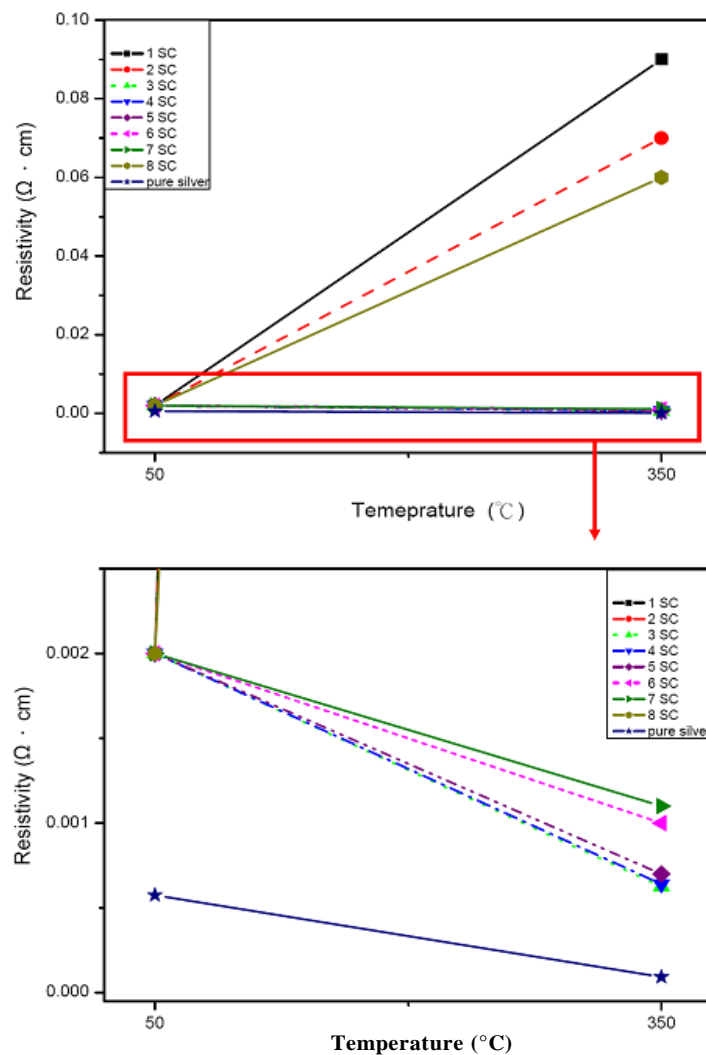


Figure 10. Resistivity variations of printed patterns as function of heat-treatment temperature. The pattern with a size of $10 \times 10 \text{ mm}^2$ were screen printed with $50 \text{ }\mu\text{m}$ thickness and head in ambient air.

and pure silver decreased drastically, but 1 SC, 2 SC and 8 SC were increased after heat treatment at 350 °C 4 hrs. As presented by the aforementioned results of XRD analysis, 1 SC, 2 SC and 8 SC have clear Cu₂O and CuO phase. The results indicated that Cu-Ag particles with incomplete silver cover layer cannot have enough prevention for oxidation of core Cu and this can cause the film resistivity to increase. Thus, after 350°C heat treatment for 4 h, Cu-Ag powders with [SC]/[Cu]= 0.25/1 and [SC]/[Ag]=8/1 have a closer resistivity ($6.25 \times 10^{-4} \Omega \cdot \text{cm}$) as pure Ag, and no Cu₂O and CuO phase were observed.

Conclusion

Cu-Ag particles with high oxidation resistance were successfully fabricated by a simple green electroless plating technique. The Ag coating on Cu surface was improved by adding SC. SEM observations which shows that the Cu-Ag composite powders do have clear core-shell structure. In the synthesized process, hindrance of SC played an important role in avoiding aggregation of Cu and synthetic Cu-Ag powders through -COOH bonding with powders. As the molar ratio of [SC]/[Cu]=0.25 and [SC]/[Ag]=8, a dense Ag coating was obtained on the Cu surface. After 350°C 4 h heat treatment, the synthetic particles with only 34.61 wt% Ag has closer resistivity ($6.25 \times 10^{-4} \Omega \cdot \text{cm}$) as pure Ag ($9.25 \times 10^{-5} \Omega \cdot \text{cm}$) which was measured, and no CuO (-1 1 1) and Cu₂O (1 1 1) peaks were detected.

ACKNOWLEDGEMENT

The financial support for this research was provided by the Industrial Development Bureau, Ministry of Economic Affairs of the Republic of China (Taiwan) under Grant no. M10000121-222 in the Conventional Industry Technology Development (CITD) program.

REFERENCES

- Athanassiou EK, Grass RN, Stark WJ (2006). Large-scale production of carbon-coated copper nanoparticles for sensor applications. *Nanotechnology* 17: 1668.
- Boca SC, Farcau C, Astilean S (2009). The study of Raman enhancement efficiency as function of nanoparticle size and shape. *Nucl. Instrum. Methods Phys. Res., B* 267: 406-410.
- Djokić S (2008). Synthesis and Antimicrobial Activity of Silver Citrate Complexes. *Bioinorg. Chem. Appl.*, p. 436458.
- Feldstein N (1981). Electrolessly fabricated product of non-catalytic metal or alloy. US Patent No. 4,305,997.
- Gils PS, Ray D, Sahoo PK (2010). Designing of silver nanoparticles in gum arabic based semi-IPN hydrogel. *Int. J. Biol. Macromol.*, 46: 237-244.
- Hackley VA (1997). Colloidal Processing of Silicon Nitride with Poly(acrylic acid): I. Adsorption and Electrostatic Interactions. *J. Am. Ceram. Soc.*, 80: 2315-2325.
- Hai HT, Ahn JG, Kim DJ, Lee JR, Chung HS, Kim CO (2006). Developing process for coating copper particles with silver by electroless plating method. *Surf. Coat. Technol.*, 201: 3788-3792.
- Hiemenz PC (1986). Principle of colloid and surface chemistry, second edition. Marcel Dekker, New York, pp. 679-729.
- Kumar M, Reddy GB (2010). Effect of atmospheric exposure on the growth of citrate-capped silver nanoparticles. *Phys., E* 42: 1940-1943.
- Lee Y, Choi J, Lee KJ, Stott NE, Kim D (2008). Large-scale synthesis of copper nanoparticles by chemically controlled reduction for applications of inkjet-printed electronics. *Nanotechnology*, 19: 415604.
- Mancier V, Rousse-Bertrand C, Dille J, Michel J, Fricoteaux P (2010). Sono and electrochemical synthesis and characterization of copper core-silver shell nanoparticles. *Ultrason Sonochemistry*, 17: 690-696.
- Park BK, Kim D, Jeong S, Moon J, Kim JS (2007). Direct writing of copper conductive patterns by ink-jet printing. *Thin Solid Films*, 515: 7706-7711.
- Ranu BC, Saha A, Jana R (2007). Microwave-Assisted Simple and Efficient Ligand Free Copper Nanoparticle Catalyzed Aryl-Sulfur Bond Formation. *Adv. Synth. Catal.*, 349: 2690-2696.
- Teramoto M, Sakaida Y, Fu SS, Ohnishi N, Matsuyama H, Maki T, Fukui T, Arai K (2000). An attempt for the stabilization of supported liquid membrane. *Sep. Purif. Technol.*, 21: 137-144.
- Takeshima E, Takatsu K, Kojima Y, Fujii T (1990). Electroplating of fine particles with metal. US Patent pp. 4,954,235.
- Vaskelis A, Matulionis E, Norkus E, Jagminiene A, Juskenas R (1996). Structure of electroless silver coatings obtained using cobalt(II) as reducing agent. *Surf. Coat. Technol.*, 82: 165-168.
- Wang B, Ji Z, Zimone, FT, Janowski GM, Rigsbee JM (1997). A technique for sputter coating of ceramic reinforcement particles. *Surf. Coat. Technol.*, 91: 64-68.
- Xu X, Luo X, Zhuang H, Li W, Zhang B (2003). Electroless silver coating on fine copper particle and its effects on oxidation resistance. *Mater. Lett.*, 57: 3987-3991.
- Yang Z, Qian H, Chen H, Anker JN (2010). One-pot hydrothermal synthesis of silver nanowires via citrate reduction. *J. Colloid Interface Sci.*, 352: 285-291.